

Electrochromic and Electrofluorochromic Performance of Novel Polysiloxane bearing Tetraaniline and Fluorescein Groups

Yang Yimeng, Chao Danming*

College of Chemistry, Jilin University, Changchun, 130012, P.R. China.

*E-mail: chaodanming@jlu.edu.cn

Received: 3 May 2020 / Accepted: 28 June 2020 / Published: 10 August 2020

Color and fluorescence dual-switching materials have recently attracted considerable attention of researchers, primarily because of their unique features in practical applications such as smart sensors, intelligent displays, multipurpose optical devices, and so on. Herein, a novel networked polysiloxane bearing tetraaniline and fluorescein groups (PSTF) was designed and synthesized via electrochemistry-assisted hydrolytic crosslinking reaction. The obtained porous interpenetrating PSTF film revealed expected electrochromic properties with clear color change, quick switching response, and acceptable coloration efficiency. By virtue of energy transfer between electroactive tetraaniline and photoluminescent fluorescein, PSTF film exhibited obvious fluorescent switching behavior under the applied potentials. Furthermore, the fluorescence switching upon acid/base substance was also revealed and investigated, ascribed to the variable molecular structure of PSTF.

Keywords: electrochromic; electrofluorochromic; polysiloxane; oligoaniline

1. INTRODUCTION

Polymeric electrochromic materials have attracted considerable interest from academia and industries because of their controllable electrochemical behavior (redox potentials), tunable optical/colorimetric properties, and excellent processability [1-5]. Thereinto, polyaniline (PANI) is one of the most promising electrochromic polymers due to its multi-colors, low switching voltage, and reversible redox transition [6-10]. To expand its practical applications, researchers have recently integrated the electrochromic feature of PANI with smart sensors, biological information storage, and intelligent display devices [11-15]. For instance, an electrochromic indicator solar cell through integrating energy storage and electrochromism functions was designed and prepared using conductive PANI nanowires as electrode material [13]. A portable lightweight integrated sensor was developed involving a piezoresistive pressure sensor, electrochromic display with Prussian blue/polyaniline coating, and a coin cell battery [14]. Although some subtle devices featuring electrochromism have been

fabricated and developed, it remains an urgent need to explore more multifarious materials for advanced intelligent applications.

Recently, our group has made considerable effect toward the enrichment of PANI's functionality through the multifunctional integration strategy. Some hydrophilic, pigmental, electroactive, and large steric hindrance groups were introduced into the molecular architecture of PANI-based electrochromic materials [16-18]. These resultant multifunctional PANI-based polymers exhibit improved electrochromic parameters in terms of fast switching speed, more coloration, long lifetime, and/or switching voltages. Nevertheless, PANI-based electrochromic polymers featuring new capacities are still exploring to expand their practical applications.

Electrofluorochromic polymers have recently gained great exposure due to their fascinating fluorescence switching properties upon the voltage [19-21]. By virtue of subtle molecular designing and tailoring, electrofluorochromic polymers would be developed based on electrochromic polymers coupled with fluorophore groups [22-24]. As a result, a series of electrochromic/electrofluorochromic dual-switching polymers have been designed and synthesized bearing electroactive and fluorescence emission groups [22-24]. Thereinto, PANI-based electrochromic/electrofluorochromic dual-switching polymers exhibit promising properties because of their low switching voltages and reversible redox transition [25,26]. Nevertheless, the fluorescence switching performance should be improved for their further application

Fluorescein is a frequently used fluorescent dye for bioscience, optics, materials science, and synthetic chemistry, due to its high fluorescent efficiency [27-31]. Taking advantage of the electrochromic properties of oligoaniline and high fluorescent efficiency of fluorescein, we surmised that a novel polymer bearing oligoaniline and fluorescein groups could exhibit reversible switch of fluorescence emission under applied potentials. Herein, a novel crosslinking network polymer containing tetraaniline and fluorescein groups was synthesized via electrochemistry-assisted hydrolytic crosslinking reaction. Its color and fluorescence switching behaviors were achieved by tunable electrochemical signals and chemical substances.

2. EXPERIMENTAL SECTION

2.1. Chemicals and solvents

3-(Triethoxysilyl)propyl isocyanate (TESPI, 99%), 5-aminofluorescein (99%), and *N*-phenyl-*p*-phenylenediamine (98%) were purchased from Aladdin. *N,N'*-Dimethylacetamide (DMAc, 99%), ethanol (99.7%), ferric trichloride (99%), and potassium carbonate (99%) were purchased from Shenyang Chemical Factory. Indium-Tin Oxide (ITO) material ($< 15 \Omega/\square$) was provided from Xiang Science & Technology Co. Ltd.

2.2. Instruments and apparatus

The molecular structure of functionalized siloxanes was verified using ^1H nuclear magnetic

resonance spectra ($^1\text{H NMR}$) on a VARIAN-300 spectrometer with the assistance of deuterated solvents. Fourier transform infrared spectroscopy (FTIR) was performed and spectra of PSTF and its precursor materials were collected using BRUKER VECTOR 22 Spectrometer. The electrochemical properties of PSTF including cyclic voltammetry (CV) and electrochemical impedance spectroscopy (EIS) were investigated using CHI 660E Electrochemical Workstation (CH Instruments, USA) with the acid electrolyte solution. The three-electrode cell consists of Ag/Ag^+ reference electrode, Pt wire counter electrode, and PSTF/ITO working electrode, respectively. The morphology change of PSTF film during the hydrolysis reaction using was monitored by field emission scanning electron microscopy (SEM, FEI Nova NanoSEM 450). Fluorescence switching behavior of PSTF film was monitored using F97Pro fluorospectro photometer (Lengguang, Shanghai). UV-3101 PC Spectrometer (SHIMADZU) was employed to monitor the optical change of UV-vis spectra under the applied potentials.

2.3. Synthesis of polysiloxane bearing tetraaniline and fluorescein groups

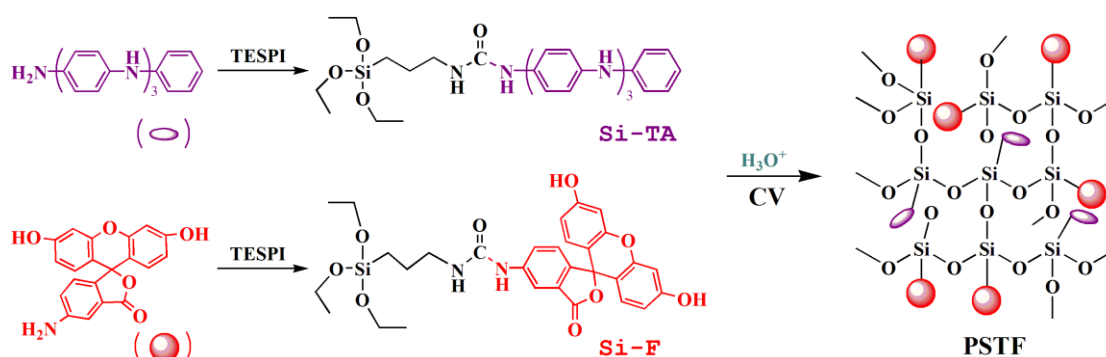
According to the previous method [32], the electroactive tetraaniline was prepared by dimerizing of *N*-phenyl-*p*-phenylenediamine under the oxidation of FeCl_3 in 1.0 M HCl solutions. After 3 h stirring, the crude product was then obtained by filtration. The crude product was reduced using 0.5 M hydrazine hydrate ammonium hydroxide solution (1.0 M) and then rinsed by water. The resulting product was dried under the vacuum with a yield of 92%.

As shown in Scheme 1, equimolar tetraaniline (0.1099 g) and TESPI (0.0742 g) were dissolved in dimethylsulfoxide (DMSO) with the nitrogen protection. The resultant solution was maintained at 80°C with continuous stirring. After 4 hours, the resulting siloxane monomer functionalized by tetraaniline group was defined as Si-TA. Considering to the hydrolytic essence of siloxane, a small quantity of Si-TA was prepared in the deuterated dimethylsulfoxide. The obtained solution was utilized for the NMR test. $^1\text{H NMR}$ ($\text{DMSO-}d_6$): $\delta = 8.11$ ppm (s, due to $-\text{CONH}-$), $\delta = 7.92\text{--}7.68$ ppm (m, due to $-\text{NH}-$), $\delta = 7.35\text{--}6.75$ ppm (m, due to Ar-H), $\delta = 6.04$ ppm (m, due to $-\text{CONH}-$), $\delta = 3.76$ ppm (m, due to $-\text{O-CH}_2-$ from ethoxy groups), $\delta = 3.02$ ppm (m, due to $-\text{CH}_2-$ next to $-\text{NH}-$), $\delta = 1.47$ ppm (m, due to $-\text{CH}_2-$), $\delta = 1.13$ ppm (m, due to $-\text{CH}_3$ from ethoxy groups), $\delta = 0.56$ ppm (m, due to $-\text{CH}_2\text{-Si(-O-)}_3$).

Equimolar 3-(triethoxysilyl)propyl isocyanate (0.2969 g) and 5-aminofluorescein (0.4168 g) were mixed in dimethylsulfoxide with the nitrogen protection. The solution was maintained at 80°C with continuous stirring. After 4 hours, the resulting siloxane monomer functionalized by fluorescein groups was defined as Si-F. Similarly, a small quantity of Si-F was synthesized in the deuterated dimethylsulfoxide. And the resultant Si-F solution was utilized for the NMR test. $^1\text{H NMR}$ ($d_6\text{-DMSO}$): $\delta = 8.25$ ppm (s, due to $-\text{CONH}-$), $\delta = 7.19\text{--}6.76$ ppm (m, due to Ar-H), $\delta = 5.76$ ppm (m, due to $-\text{CONH}-$), $\delta = 3.75$ ppm (m, due to $-\text{O-CH}_2-$ from ethoxy groups), $\delta = 2.96$ ppm (m, due to $-\text{CH}_2-$ next to $-\text{NH}-$), $\delta = 1.40$ ppm (m, due to $-\text{CH}_2-$), $\delta = 1.08$ ppm (m, due to $-\text{CH}_3$ from ethoxy groups), $\delta = 0.53$ ppm (m, due to $-\text{CH}_2\text{-Si(-O-)}_3$).

A precursor mixture solution was formed using Si-TA and Si-F DMSO solutions with stirring under nitrogen protection. After 1 h, the precursor mixture solution was drop-casted on the clean surface of ITO, which was cleaned with alcohol, acetone, and water using the ultrasound method. A dried

precursor mixture film was formed after heating under the vacuum at 40°C. A three-electrode cell system was fabricated for the electrochemistry with the above precursor mixture decorated electrode, Ag/Ag⁺ electrode, and Pt electrode. Then the CV model was run in the voltage of 0~1.0 V at 0.1 V/s in 0.1 M HCl electrolyte solution. 25 CV cycles later, a crosslinked network polysiloxane was synthesized through the hydrolytic reaction as shown in Scheme 1. The resultant polymer is defined as PSTF. The as-fabricated PSTF/ITO electrodes are ready to use in the following electrochemical measurements.



Scheme 1. Synthetic route of PSTF.

3. RESULTS AND DISCUSSION

3.1. Synthesis and characterization of PSTF

Firstly, the nucleophilic reaction was carried out between isocyanate and amine groups under nitrogen protection. The functionalized siloxane monomers solution was formed with stirring at room temperature. The ¹H NMR spectra of the resultant functionalized siloxane monomers were provided in Figure 1. The signals from the ethoxy group appear at 3.7 ppm and 1.1 ppm. The methylene groups show multiple signal peaks around 3.0 ppm, 1.5 ppm, and 0.5 ppm, respectively. As shown in Figure 1, Si-TA shows characteristic uramido signal peaks at 8.11 ppm and 6.04 ppm, indicating the accomplishment of nucleophilic reaction between isocyanate and amine groups. Other signal peaks in the region of 7.35-6.75 ppm are ascribed to the aryl groups from tetraaniline. Moreover, the amine groups from tetraaniline segments show characteristic signal peaks centered at 7.92 and 7.68 ppm. Si-F precursor exhibits the signal peaks of uramido groups around 8.25 and 5.76 ppm. In addition, the signals of aryl groups from fluorescein appear around 7.19-6.76 ppm. All the NMR signal peaks in Figure 1 are in accordance with the expected molecular structure of the functionalized siloxane monomers.

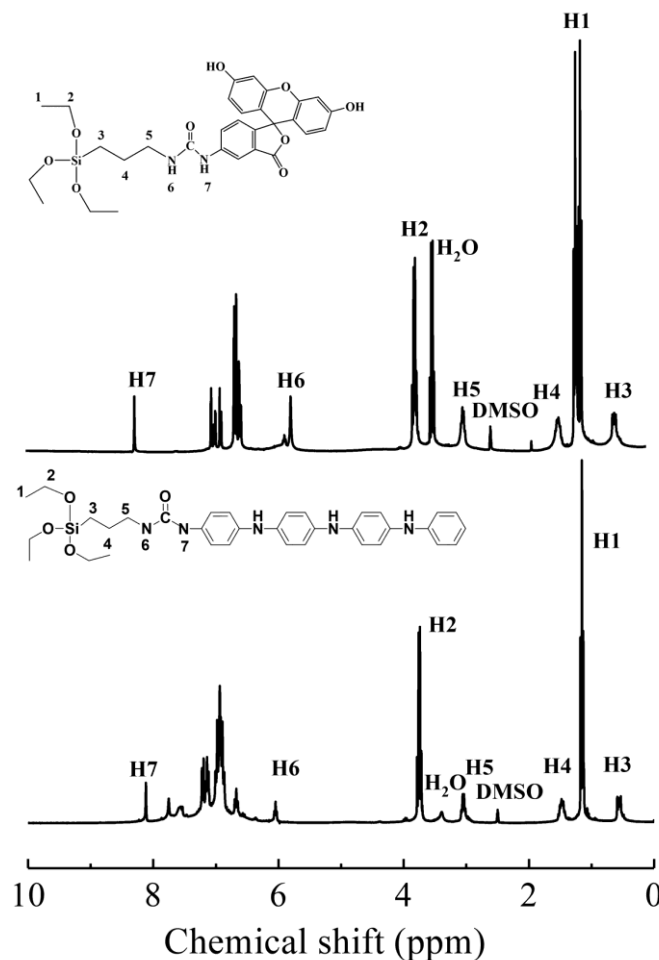


Figure 1. ¹H NMR spectra of Si-TA and Si-F.

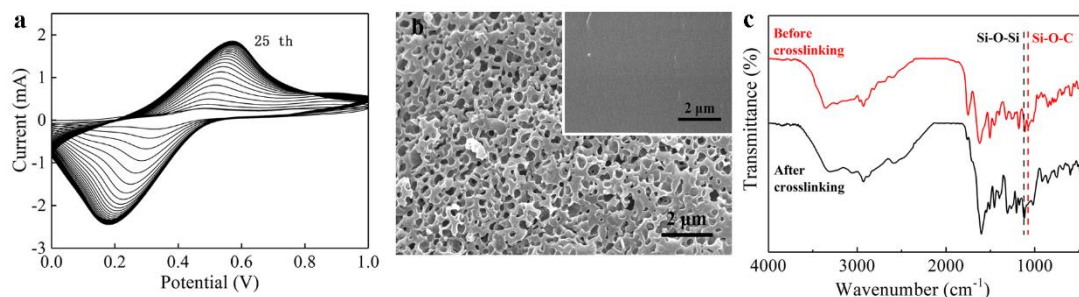


Figure 2. (a) CV curves of siloxane precursors mixture in the potential range of 0~1.0 V at 100 mV/s. (b) SEM morphology of PSTF after hydrolysis, and the inset shows the SEM morphology of siloxane precursors mixture before hydrolysis. (c) FTIR spectra of siloxane precursors mixture and PSTF.

The crosslinking reaction proceeded among the siloxane precursors through hydrolysis in the solid state using electrochemistry. This hydrolysis of siloxane precursors was triggered by H_3O^+ , which could insert and/or extract through the PSTF coating upon the applied electrokinetic voltages. The

hydrolytic crosslinking process was responded to the CV curves in Figure 2a. With the undergoing of hydrolytic crosslinking reaction, the peak currents of CV switching increase gradually and reach maximum value after 25 cycles. The resultant electroactive film exhibits the same CV curves without any change in the following switching, indicating the completion of hydrolysis in the solid coating. Also, SEM was also used to study the hydrolytic crosslinking reaction. The inset of Figure 2b shows uniform, smooth, and compacted morphology on the surface of the precursor mixture film. After 25 CV cycles, the surface of the working electrode shows uniform interpenetrating network morphology. This loosened porous interpenetrating structure would be attributed to the molecular segment aggregation and small molecules release stemmed from the hydrolysis of siloxane precursors.

The molecular structure change before/after hydrolysis was investigated using FTIR spectra (in Figure 2c). Both of the FTIR spectra display the characteristic N–H stretching vibration around 3363 cm^{-1} , and alkyl C–H stretching vibration at 2836 cm^{-1} , respectively. The peaks at 1301 cm^{-1} and 1203 cm^{-1} are ascribed to the stretching vibrations of C–N groups and deformation vibration of Si–C groups. Before crosslinking, the siloxane precursors mixture shows the stretching vibration of Si–O–C at 1074 cm^{-1} . While PSTF shows obvious Si–O–Si stretching vibration around 1118 cm^{-1} after hydrolysis. Obviously, all the Si–O–C bonds convert into Si–O–Si bonds after the hydrolytic crosslinking reaction.

3.2. Electrochemical properties

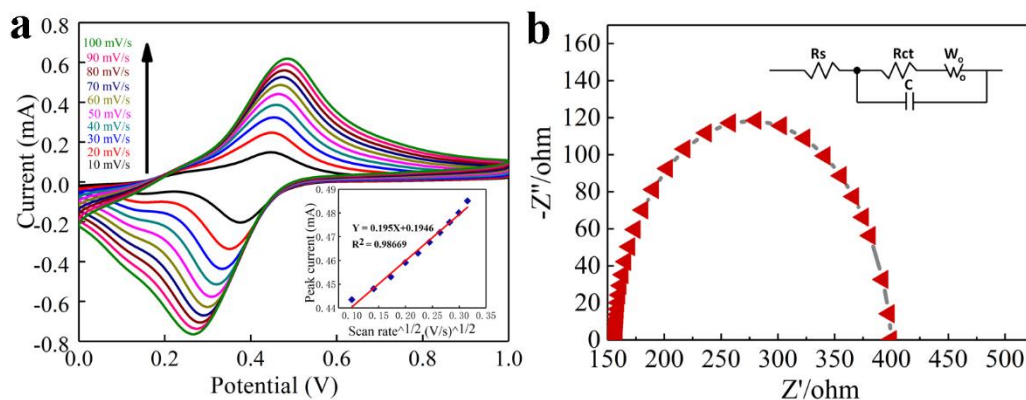


Figure 3. (a) CV curves of PSTF in a potential range of 0~1.0 V at various scan rates from 10 to 100 mV/s. The inset shows the relationship curve between the peak current and the square root of the scan rate. (b) EIS of PSTF in 0.1 M HCl electrolyte solution.

CV measurements were performed on PSTF/ITO electrode with scan rates of 10~100 mV/s. The applied voltage switched from 0 V to 1.0 V. One couple of redox peaks are disclosed at 0.48 V/0.26 V during the CV process in Figure 3a, due to the reduced/oxidized transition of tetraniline. Usually, PANI and its derivatives show two pairs of redox peaks during the CV switching, indicating three redox states in their conjugated molecular structure. Obviously, the vanishment of intermediate emeraldine state of PSTF in the CV curve should be a kinetic phenomenon, indicating that the redox transition of the tetraaniline segments can not keep up with the variation of voltage during the CV process. This hysteresis should be due to its poor conductivity and the crosslinked networked molecular architecture. Moreover,

the relationship between peak currents and scan rates is also depicted as shown in the inset of Figure 3a. A linear correlation between the peak current and the square root of the scan rate is determined, indicating a diffusion-controlled process. The charge transfer resistance (R_{ct}) of PSTF was also studied using EIS (Figure 3b). Here the Randles type equivalent circuit model was utilized to fit the Nyquist plots. According to the intersection of the low-frequency end of the semicircle arc with the real axis, the R_{ct} value is about 400 Ω , which should be ascribed to its porous interpenetrating microstructure.

3.3. Electrochromic behavior

The electrochromic behavior of the obtained PSTF was studied on an electrochemical workstation coupled with UV-Vis spectroscopy. The applied voltages on the PSTF/ITO electrode were fixed at 0 V, 0.2 V, 0.4 V, 0.6 V, 0.8 V, and 1.0 V, respectively. All the transmittance spectra of electrochromic electrode were collected and presented in Figure 4a. With the applied voltage increasing, the absorbance in the range of 500~800 nm increases accordingly with a visible color change from gray to yellow-green, and finally to dark green. The color of PSTF/ITO electrode was recorded by the camera as shown in the inset of Figure 4a. It is obvious that this electrochromic feature should stem from the redox transition of tetraaniline moieties. The optical contrast of PSTF film during the electrochromic process is calculated about 35% at 750 nm from 0 V to 0.6 V. Moreover, the color change of PSTF film is also described using the color coordinates as shown in Fig. 4b. The color coordinates of PSTF film are CIE 1931: x, 0.3210; y, 0.3401 at 0 V (transparent gray), CIE 1931: x, 0.3451; y, 0.4622 at 0.4 V at 0.4 V (yellow-green), and CIE 1931: x, 0.2933; y, 0.5861 at 0.8 V at 0.8 V (dark green), respectively. It is much different from the color change of the pure PANI in the electrochromism (from gray to green, and blue) [6-8]. It is obvious that the resultant color change in a wide color region should be attributed to the involvement of fluorescein groups.

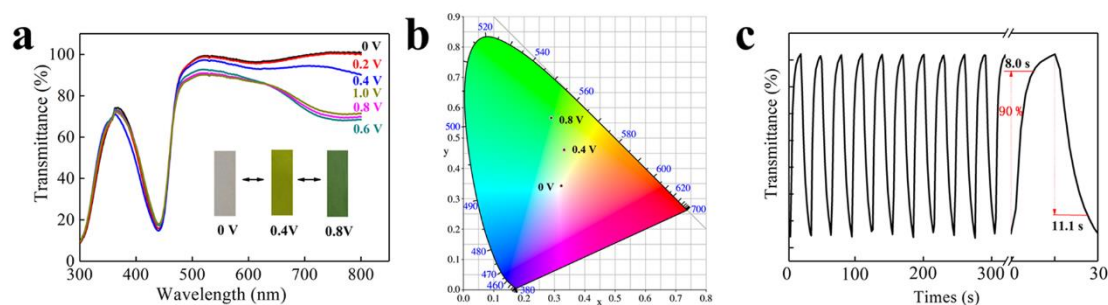


Figure 4. (a) Transmittance spectra of PSTF film under various voltages with a residence time of 200 s. Inset reveals the photographs under various applied voltages. (b) The CIE 1931(x, y) chromaticity diagram of the PSTF films at different potentials. (c) Optical change of PSTF film collected at 750 nm under voltages of 0 V and 0.6 V, and its switching times during the color switching.

The spectrochronoamperometry measurements have also been run on the PSTF coating under

alternative voltages of 0 V and 0.6 V with the residence time of 15 s. Transmittance change at 750 nm was collected and presented in Figure 4b. From the transmittance difference value, current consumption, as well as active area, the coloration efficiency value of PSTF was calculated about $80.4 \text{ cm}^2/\text{C}$, which is higher than other reported materials, such as PE-co-M2 ($69.23 \text{ cm}^2/\text{C}$) [33], PEDOS ($79.2 \text{ cm}^2/\text{C}$) [34], and WO_3/PANI nanorod arrays compared ($76 \text{ cm}^2/\text{C}$) [35]. Besides, the switching time was also determined from these transmittance change curves. The PSTF/ITO electrode exhibits moderate switching times of 11.1 s/8.0 s for the coloring/bleaching process.

3.4. Electrofluorochromic properties

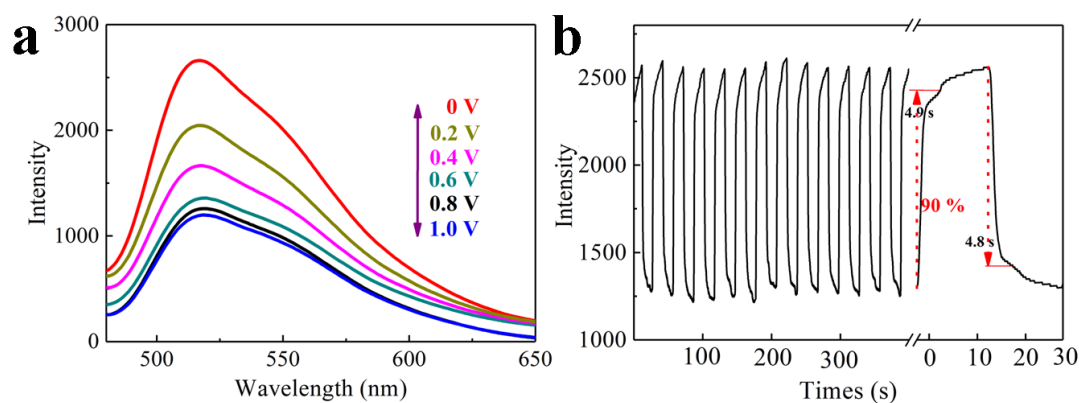


Figure 5. (a) Fluorescence spectra of PSTF film under various voltages (0.0-1.0 V). (b) Fluorescence change at 517 nm of PSTF coating under repeated applied voltages of 0 V and 1.0 V. The excitation wavelength is fixed at 425 nm.

Optical materials featuring tunable fluorescence have attracted great interest because of wide applications of smart sensors, high-quality displays, and intelligent photovoltaic conversion appliances. Because of their rapidity, convenience, and availability, the electrical signals are regarded as promising candidates to adjust the fluorescence properties. The resultant PSTF bearing fluorophore and electroactive units could display switching fluorescence upon the repeat electrical signals. Hence, the spectroelectrochemical measurements carried out on PSTF coating through an electrochemical workstation coupled with fluorospectro photometer. The fluorescence spectra of PSTF film were obtained under different voltages of 0 V, 0.2 V, 0.4 V, 0.6 V, 0.8 V, and 1.0 V, respectively (Figure 5a). The residence time is 200 s. With the increase of voltage, PSTF shows decreasing fluorescence intensity. When the applied voltage is 1.0 V, the PSTF/ITO electrode shows 45% of fluorescence intensity value (0 V). The reversibility of fluorescence intensity upon the applied voltages is verified in the spectroelectrochemical measurements. The energy transfer and interplay between tetraaniline and fluorescein units should be responsible for this typical electrofluorochromic feature. These quinoid structures in oxidative tetraaniline, as the excitation traps, would quench the fluorescence due to their short-lived excited state essence [33,37]. In addition, the spectrochronoamperometry measurements strategy was also executed on PSTF/ITO electrode. The fluorescence intensity change at 517 nm is collected and presented in Figure 5b. The repeated applied voltages are 0 V and 1.0 V. The residence

time is 15 s. The typical fluorescence switching curves reveals short switching times of 4.9 s/4.8 s for its on/off states, which is shorter than electrofluorochromic materials such as PAAK-tBu-CzTPA (4.42 s/6.2 s) [38] and PUOT (9.4 s/10.8 s) [25].

3.5. Fluorescence switching behavior upon acid/base substance

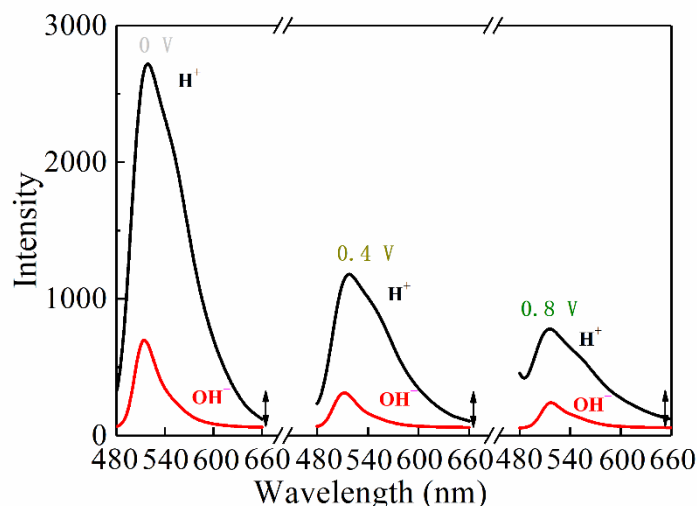


Figure 6. Fluorescence switching of PSTF/ITO electrode when immersed into the acid solution and alkaline solution alternately. The redox state of tetraaniline units in PSTF structure was fixed by the potentiostatic method at voltages of 0 V, 0.4 V, and 0.8 V.

H^+/OH^- ions should be used as the stimuli for the spectroscopic changing of PSTF because of the reversible protonation/deprotonation behavior of polyaniline-type materials. Here, we also explored the fluorescence change of PSTF in different acid and base environments under stationary electrochemical oxidation. The fluorescence changing properties upon acid/base stimuli was collected on PSTF/ITO electrode using fluorospectro photometer coupled with an electrochemical workstation. Here the potentiostatic method was run to fix the redox states of tetraaniline with a residence time of 200 s. 0.1 M HCl solution is used as the electrolyte in this measurement. The alkaline solution is 0.1 M NaOH solution. Tetraaniline in PSTF structure is fixed in the reduced state, intermediate oxidation state, and highest oxidation state, respectively, when the applied voltages were fixed at 0 V, 0.4 V, and 0.8 V. As the applied voltage was 0.4 V, the fluorescence intensity of PSTF/ITO film decreased to 44% of the initial fluorescence intensity (at 0.0 V). When the voltage was elevated to 0.8 V, the fluorescence intensity decreased to 28% of its initial value (at 0.0 V). Next, the PSTF/ITO films in different oxidized states were immersed into a 0.1 M NaOH solution for 2 min. After the immersion of the NaOH solution, its fluorescence intensity continues to decrease. This reversible fluorescence change upon the H^+/OH^- ions stimuli could be attributed to the protonation/deprotonation effect of tetraaniline as follow. As immersed in a 0.1 M HCl solution, the amine groups in tetraaniline would be protonated by H^+ ions. This protonated tetraanilines could dramatically alter their molecular structure and interchain interaction, resulting in enhanced fluorescence intensity. As immersed in an alkaline solution, the OH^- ions would

neutralize the H^+ ions immediately. This deprotonation effect could bring back the pristine molecular structure of tetraaniline, resulting in a fluorescence quenching phenomenon. As shown in Figure 6, the PSTF film would display a decreased fluorescence intensity (26%), as the tetraaniline changes from leucoemeraldine salt state to LEB due to the deprotonation effect (at 0.0 V). Similarly, the fluorescence intensity of PSTF/ITO electrode reduces to 25% when the tetraaniline changes from emeraldine salt state to EB due to the deprotonation effect (at 0.4 V). As the voltage was fixed 0.8 V, the fluorescence intensity of PSTF film reduces to 31% with the tetraaniline segments changing from pernigraniline salt state to PNB. Moreover, the structure change of fluorescein groups in acid/base solution would be another important influence factor because of variable phenolic hydroxyl groups. The investigation of the effect of phenolic hydroxyl structure on fluorescence intensity is still undergoing in our lab.

4. CONCLUSIONS

We prepared a novel network polysiloxane containing tetraaniline and fluorescein groups via electrochemistry-assisted hydrolytic crosslinking reaction. The color and fluorescence of this crosslinking network PSTF film can be effectively adjusted by electrochemical potentials, showing the dual electrochromic and electrofluorochromic performance. Due to its variable molecular structure, PSTF film also exhibits fluorescence switching upon acid/base substance. This multi-functional polymer is the beginning of our exploitation in the color/fluorescence dual-switching area. Further work would be the development of this type of material to the biosensors and intelligent displays.

ACKNOWLEDGEMENTS

We graciously acknowledge the National Natural Science Foundation of China for funding (grant No. 21774046) and Jilin Provincial Science and Technology Department, China (Grant Nos. 20190201075JC and 20200801057GH).

NOTES

The authors declare no competing financial interest.

References

1. X. Li, K. Perera, J. He, A. Gumyusenge and J. Mei, *Journal of Materials Chemistry C*, 7 (2019) 12761.
2. P. Zhang, X. Xing, Y. Wang, I. Murtaza, Y. He, J. Cameron, S. Ahmed, P.J. Skabara and H. Meng, *Journal of Materials Chemistry C*, 7 (2019) 9467.
3. Z. Xu, L. Kong, Y. Wang, B. Wang and J. Zhao, *Organic Electronics*, 54 (2018) 94.
4. C.-R. Zhu, J.-P. Xie, H.-R. Mou, Z.-J. Huang, Q. Tang, C.-B. Gong and X.-K. Fu, *New Journal of Chemistry*, 43 (2019) 13654.
5. G.W. Kim, Y.C. Kim, I.J. Ko, J.H. Park, H.W. Bae, R. Lampande and J.H. Kwon, *Advanced Optical Materials*, 6 (2018) 1701382.
6. Y. Zhao, S. Zhang, F. Hu, J. Li, H. Chen, J. Lin, B. Yan, Y. Gu and S. Chen, *Journal of Materials Science: Materials in Electronics*, 30 (2019) 12718.
7. L. Zhang, B. Wang, X. Li, G. Xu, S. Dou, X. Zhang, X. Chen, J. Zhao, K. Zhang and Y. Li, *Journal of Materials Chemistry C*, 7 (2019) 9878.

8. L. Zhao, L. Zhao, Y. Xu, T. Qiu, L. Zhi and G. Shi, *Electrochimica Acta*, 55 (2009) 491.
9. P. Foot and R. Simon, *Journal of Physics D: Applied Physics*, 22 (1989) 1598.
10. C.-H. Yang, Y.-K. Chih, W.-C. Wu and C.-H. Chen, *Electrochemical and Solid State Letters*, 9 (2005) C5.
11. Y. Zhou, E.B. Berda, Q. Ma, X. Liu, C. Wang and D. Chao, *ChemElectroChem*, 6 (2019) 5293.
12. M. Porcel-Valenzuela, J. Ballesta-Claver, I. de Orbe-Payá, F. Montilla and L.F. Capitán-Vallvey, *Journal of Electroanalytical Chemistry*, 738 (2015) 162.
13. K. Wang, H. Wu, Y. Meng, Y. Zhang and Z. Wei, *Energy & Environmental Science*, 5 (2012) 8384.
14. D.D. Liana, B. Raguse, J.J. Gooding and E. Chow, *Advanced Materials Technologies*, 1 (2016) 1600143.
15. J.-C. Chou, C.-Y. Liu, C.-J. Yang, Y.-H. Liao, M.-W. Su and C.-C. Chen, *Journal of Display Technology*, 11 (2015) 443.
16. Y. Li, Y. Zhou, X. Jia, X. Liu, C. Wang and D. Chao, *Journal of Polymer Science Part A: Polymer Chemistry*, 56 (2018) 412.
17. D. Chao, T. Zheng, H. Liu, R. Yang, X. Jia, S. Wang, E.B. Berda and C. Wang, *Electrochimica acta*, 60 (2012) 253.
18. Y. Li, X. Jia, Y. Zhou and D. Chao, *Express Polymer Letters*, 12 (2018) 649.
19. H. Al-Kutubi, H.R. Zafarani, L. Rassaei and K. Mathwig, *European Polymer Journal*, 83 (2016) 478.
20. S. Seo, H. Shin, C. Park, H. Lim and E. Kim, *Macromolecular Research*, 21 (2013) 284.
21. P. Audebert and F. Miomandre, *Chemical Science*, 4 (2013) 575.
22. S. Mi, J. Wu, J. Liu, Z. Xu, X. Wu, G. Luo, J. Zheng and C. Xu, *ACS Applied Materials & Interfaces*, 7 (2015) 27511.
23. N. Sun, S. Meng, D. Chao, Z. Zhou, Y. Du, D. Wang, X. Zhao, H. Zhou and C. Chen, *Polym Chem*, 7 (2016) 6055.
24. N. Sun, Z. Zhou, D. Chao, X. Chu, Y. Du, X. Zhao, D. Wang and C. Chen, *Journal of Polymer Science Part A: Polymer Chemistry*, 55 (2017) 213.
25. Y. Yan, N. Sun, X. Jia, X. Liu, C. Wang and D. Chao, *Polymer*, 134 (2018) 1.
26. Y. Li, Y. Zhou, X. Jia and D. Chao, *European Polymer Journal*, 106 (2018) 169.
27. M. Li, J. Yang, Y. Ou, Y. Shi, L. Liu, C. Sun, H. Zheng and Y. Long, *Talanta*, 182 (2018) 422.
28. G. Liu, P. Ren, F. Yang, X. Dou, J. Wang and Y. Song, *Canadian Journal of Chemistry*, 96 (2018) 1037.
29. K. Tripathi, A. Rai, A.K. Yadav, S. Srikrishna, N. Kumari and L. Mishra, *RSC advances*, 7 (2017) 2264.
30. M.A. Kramer, W.R. Tompkin and R.W. Boyd, *Physical Review A*, 34 (1986) 2026.
31. T. Moutray, M. Alarbi, G. Mahon, M. Stevenson and U. Chakravarthy, *British Journal of Ophthalmology*, 92 (2008) 361.
32. W. Zhang, J. Feng, A.G. MacDiarmid and A.J. Epstein, *Synthetic Met*, 84 (1997) 119.
33. S. Singhal, P. Yadav, S. Naqvi, S. Gupta and A. Patra, *ACS Omega*, 4 (2019) 3484.
34. P. Yadav, S. Singhal and A. Patra, *Synthetic Metals*, 260 (2020) 116264.
35. D. Ma, G. Shi, H. Wang, Q. Zhang and Y. Li, *J. Mater. Chem. A*, 2 (2014) 13541.
36. J. Thorne, J. Masters, S. Williams, A.G. MacDiarmid and R. Hochstrasser, *Synthetic metals*, 49 (1992) 159.
37. J.Y. Shimano and A.G. MacDiarmid, *Synthetic Metals*, 123 (2001) 251.
38. Y. Han, Y. Lin, D. Sun, Z. Xing, Z. Jiang and Z. Chen, *Dyes and Pigments*, 163 (2019) 40.